Strong, Twist-Stable Carbon Nanotube Yarns and Muscles by Tension Annealing at Extreme Temperatures

*Jiangtao Di, Shaoli Fang, Francisco A. Moura, Douglas S. Galvão, Julia Bykova, Ali Aliev, Mônica Jung de Andrade, Xavier Lepró, Na Li, Carter Haines, Raquel Ovalle-Robles, Dong Qian, and Ray H. Baughman**

Twist-spun carbon nanotube (CNT) yarns are of great interest for such diverse applications as artificial muscles,[1–3] supercapacitors,[4] batteries,[5,6] intelligent textiles, and structural composites.[7,8] While inserted twist can generate new properties (e.g., torsional and tensile actuation[1–3]) and improve the properties such as strength and stretchability,[9,10] single-ply twisted or coiled neat CNT yarns will irreversibly untwist unless they are torsionally tethered.[11] This problem is particularly troublesome for twist-spun CNT yarn artificial muscles that provide torsional and tensile actuation.[1,2,12] It is also a key problem for twist retention during weaving CNT yarns.

We here provide an incandescent tension annealing process (ITAP) for stabilizing both twisted and coiled CNT yarns with respect to unwanted irreversible untwist, thereby avoiding the need to tether torsional artificial muscles, and increasing the mechanical loads that can be driven by these muscles. This ITAP involves thermally annealing twisted CNT yarns at a temperature of about 2000 °C while these yarns are under tensile loads. Depending upon the density of the precursor yarn, the ITAP increased yarn modulus and yarn strength by factors of up to 12 and 2.6, respectively. While a nontethered pristine yarn immediately underwent irreversible untwist when strained by a freely rotating weight, a nontethered ITAP yarn could be reversibly actuated by cyclic vapor sorption/desorption to rotate a 6100 times heavier rotor by 52° per millimeter of muscle length, thereby achieving a peak rotation speed of 160 rpm. In addition, the ITAP conferred remarkable long-term resistance to chlorosulfonic acid whose strong protonation ability caused pristine yarns to swell, disorder, and mechanically fail within minutes.

Various important means are now available for continuously making CNT yarns by either liquid-state[13–15] or dry-state methods.[9,16–20] Yarns spun from spinnable nanotube forests have high mechanical strength, low impurity, good nanotube alignment, and novel structure flexibility,[7,9,21] which have been widely investigated for fiber devices.[1–8] Adding twist to these yarns can improve their strength[9] and enable them to work as high-strain conductors[10,22] and high-performance torsional and tensile artificial muscles.[1–3] Taking the CNT yarn artificial muscles for example, when infiltrated with electrolyte and electrochemically driven, these two-end tethered yarns could rotate a rotor at speeds exceeding 590 rpm, providing torsional strokes per yarn length of 125° mm^{-1}.[1] Twisted yarns infiltrated with volume-changing guests provided torsional speeds of up to 11 500 rpm.[2]

However, several problems still exist because of the weak interfacial connection between adjacent nanotubes within yarns.[23] First, twisted and coiled yarns snarl unless tensionally constrained. Second, single-ply twisted and single-ply coiled CNT yarn muscles must be torsionally tethered to prevent irreversible untwist and need a nonactuating segment as a returning spring for torsional actuation.[1,2] Third, the twisted yarns are still several orders of magnitude lower in strength compared to individual nanotubes.[7] These problems have limited the practical applications of CNT yarns. Therefore, increasing mechanical bonding within the yarn structure is of great importance for both twist retention and mechanical strength.

While infiltration of CNT yarns with polymers provides a well-known means to increase yarn strength, modulus, and toughness,[8,24,25] such infiltration cannot be generically applied for CNT yarn muscles, since volume changes of electrolyte or guest within the yarn drive the actuation of the yarn muscle. An alternative approach is to covalently link adjacent nanotubes, such as by using radiation.[23,26,27] Irradiating carbon double-walled nanotube (DWNT) bundles (containing dozens of' nanotubes) by an electron beam in an electron transmission microscope increased the tensile strength and elastic modulus of the individual nanotube bundle by an order of magnitude, up to maximum values of 1.5–17.1 GPa and 103–693 GPa, respectively.[28] However, application of this approach to micrometers-thick CNT yarns is practically limited by the penetration length of

Dr. J. Di, Prof. S. Fang, Prof. A. Aliev,
Dr. M. Jung De Andrade, Dr. X. Lepró, Dr. N. Li,
Dr. C. Haines, Prof. R. H. Baughman
The Alan G. MacDiarmid NanoTech Institute
University of Texas at Dallas
Richardson, TX 75080, USA
E-mail: ray.baughman@utdallas.edu
F. A. Moura, Prof. D. S. Galvão
Applied Physics Department
State University of Campinas
Campinas, SP 13081-970, Brazil
Dr. J. Bykova, Dr. R. Ovalle-Robles
Nano-Science & Technology Center
Lintec of America
Richardson, TX 75081, USA
Prof. D. Qian
Mechanical Engineering Department
University of Texas at Dallas
Richardson, TX 75080, USA

DOI: 10.1002/adma.201600628

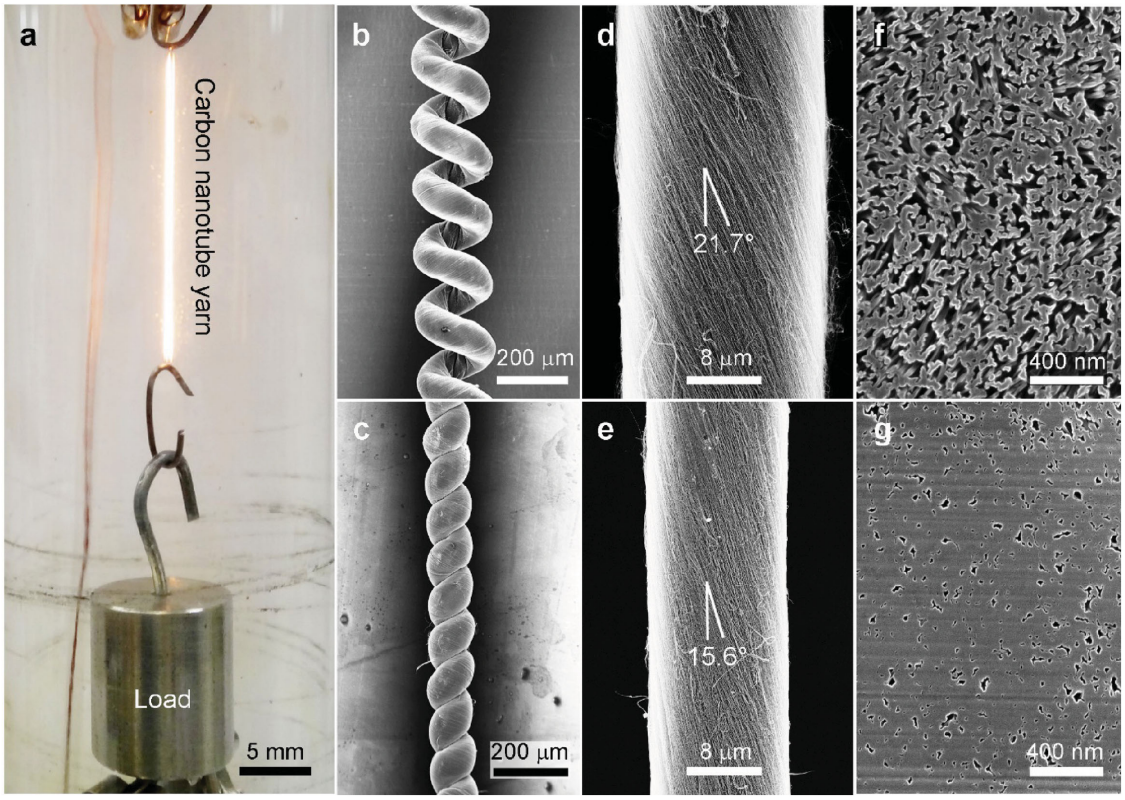

Figure 1. a) Setup for applying ITAP to MWNT yarns. SEM images of the effects of an applied freely rotating load on b) a nontethered, non-ITAP coiled yarn and c) a nontethered, coiled ITAP yarn, showing that the ITAP stabilizes the coiled yarn with respect to untwisting. d,e) SEM images and f,g) cross-sectional SEM images (areas near the midpoint of yarn radius) of a twist-spun pristine yarn having an initial density of 0.5 g cm^{-3} d,f) before and e,g) after ITAP-40, indicating the density increase by the ITAP.

electron beams. Irradiation of CNT yarns by gamma rays in the air increased strength and modulus of CNT yarns possibly due to the formation of carboxyl-like groups between adjacent nanotubes, but the final tensile strength of these irradiated yarns was only about 850 MPa.[29] Fan and co-workers has importantly shown that thermally annealing twisted CNT yarns in vacuum for several hours at 2000 K, without significant applied stress, increased Young's modulus from 37 to 74 GPa, but slightly decreased yarn strength (from 600 to 564 MPa).[19]

The presently described ITAP involved heating a vertically suspended, two-end-tethered carbon multiwalled nanotube (MWNT) yarn to about 2000 °C in vacuum by applying about 2×10^4 A cm^{-2} current while tensile stress was applied by a weight attached at the yarn end (**Figure 1**a). The applied stress is normalized as a percent Φ of the room-temperature tensile strength of precursor yarns, σ_{max}, and is designated by ITAP-Φ. The results of Figure S1 in the Supporting Information show that equivalent property improvement can be obtained by heating CNT yarns either thermally or electrothermally.

The used MWNT yarns were twist-spun from an about 250-μm-high drawable nanotube forest that was synthesized by chemical vapor deposition.[9] Transmission electron microscopy (TEM) indicates that these MWNTs contain about nine graphitic walls and have a diameter of ≈13 nm (Figure S2, Supporting Information). By using either one or two tension bars near the tip of the spinning wedge (Figure S3, Supporting Information), increased tensile stress was applied to the spinning wedge, which increased the density of the as-spun yarns and thus enabled investigation of the effects of yarn density on the mechanical properties obtained by the ITAP. The experiment results described here showed that the major property improvements were realized within a few seconds and that application of ITAP for longer than 10 min degraded strength and modulus (Figure S4, Supporting Information). Thus, unless otherwise indicated, an annealing time of 2 min was employed.

Before the ITAP, the coiled pristine nanotube yarn untwisted to a very loose spring structure when attached to a 1-MPa freely rotating load (Figure 1b) or snarled to provide a torque balanced structure when the yarn ends were not tethered (Figure S5, Supporting Information). In contrast, the ITAP coiled yarns remained straight and negligibly untwisted upon release of tethering (Figure 1c). Similar results were observed for highly twisted yarns. These observations indicate that the ITAP stabilizes the twisted and the coiled structures of CNT yarns.

The scanning electron microscope (SEM) images of Figure 1d,e show that the ITAP-40 decreased both yarn bias angle (α) and diameter (d). The results of Table S1 (Supporting Information) and the associated calculations (Supporting Information) demonstrate that the bias angles for ITAP yarns were accurately predicted from the bias angles for pristine yarns and the relative diameters of pristine and ITAP yarns by using the equation $\alpha = \tan^{-1}(\pi d T)$, where T is the inserted twist per yarn

length. High-magnification SEM images show the increase of nanotube alignment and nanotube bundle size induced by the ITAP-40 (Figure S6, Supporting Information). The cross-sectional SEM images (Figure 1f,g) provided a comprehensive observation of the decrease in yarn porosity resulted from the ITAP-40. The percentage of the void area measured from the cross-sectional images decreased from about 30% to about 15%, corresponding to the increase in average yarn density from 0.5 to 0.93 g cm^{-3}. Consistent results were observed when applying the ITAP-40 to pristine yarns having a higher density of 1.08 g cm^{-3} (Figure S7, Supporting Information). Annealing with tension did not cause obvious morphological changes of the CNT yarns but led to a slight decrease in yarn density, possibly because of carbon evaporation (Figure S7, Supporting Information).

Raman spectroscopy shows that the intensity ratio of the graphite-structure-derived G-band to the defect-derived D-band (G/D) increased with increasing annealing time (Figure S8, Supporting Information). However, the G/D ratio only increased from 1.1 to 1.3 after applying the ITAP-30 for 10 min, and this or shorter annealing time provided ITAP yarns with optimal mechanical properties (Figure S4, Supporting Information). Similarly, X-ray photoelectron spectroscopy (Figure S9, Supporting Information) and X-ray diffraction (Figure S10, Supporting Information) demonstrated only a slight structure change after applying the ITAP-40 for 2 min. TEM images show that the ITAP well maintained the tubular structures of CNTs (Figure S11, Supporting Information).

The effects of the mechanical stress applied during ITAP on the mechanical properties of twisted MWNT yarns are shown in **Figure 2**a. The pristine MWNT yarn (density: 1.08 g cm^{-3}) has a specific strength (gravimetric strength) of 0.85 N tex^{-1} and a specific modulus (gravimetric Young's modulus) of 43.2 N tex^{-1}. Annealing this yarn at 2000 °C without applying stress caused a 10% decrease in strength and a 27% increase in modulus (Figure 2a), which is consistent with the previous results.[19] However, when a tensile stress of over 20% of σ_{max} was applied, the ITAP yarns showed higher strength and modulus than the pristine yarn, and the strength and modulus increased with increasing the applied stress (Figure 2a). At the highest applied stress (40% of σ_{max}), the ITAP-40 increased specific strength, specific modulus, and density by factors of 1.65, 3, and 1.88, respectively. Nevertheless, stress applied at room temperature was not effective in significantly improving mechanical properties (Figure S12, Supporting Information). Thus, the combination of stress and high-temperature annealing is essential for improving the mechanical properties of MWNT yarns, wherein the applied stress can help align nanotubes and apply lateral compression to draw nanotubes into close proximity to participate in high-temperature-enhanced inter-nanotube connections.[19]

The results in Figure 2b,c show that tensile strength and modulus (and specific strength and specific modulus) substantially increased after ITAP-40 for all investigated precursor yarn densities. The highest-density precursor yarns

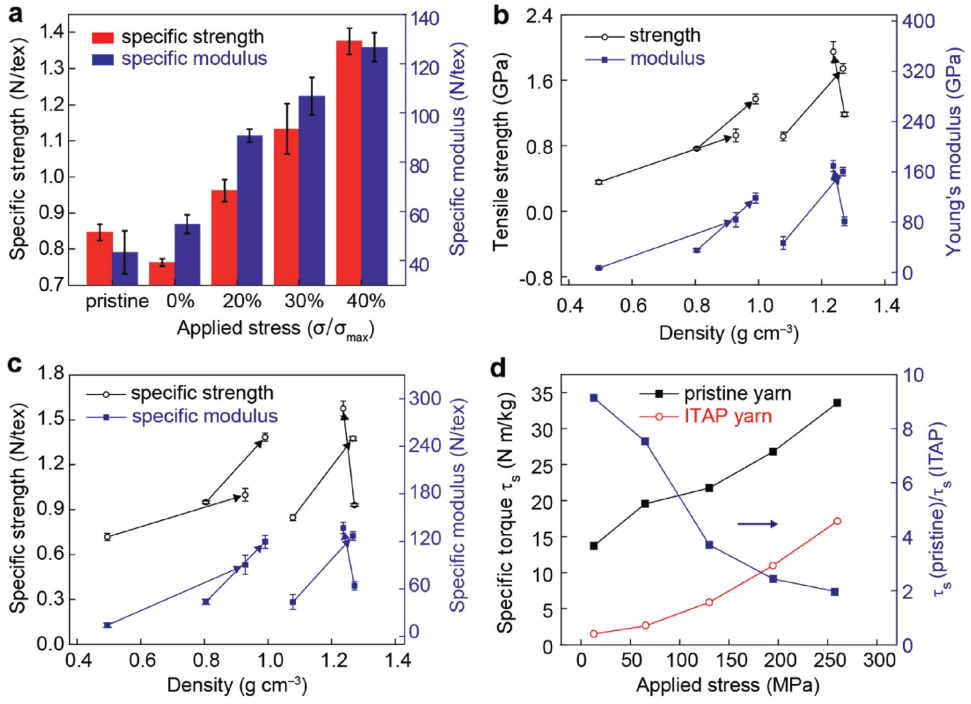

Figure 2. Mechanical properties of twisted pristine and ITAP yarns. a) Comparison of the specific strength and specific modulus of a pristine yarn (1.08 g cm^{-3} in density) and that for corresponding ITAP yarns annealed under different applied stresses, where the applied stress during ITAP (σ), is normalized to the fracture strength of the pristine yarn (σ_{max}). b) Tensile strength and Young's modulus as a function of density for pristine and ITAP-40 yarns. The arrows in panels (b) and (c) connect the mechanical property before ITAP to the corresponding mechanical property after ITAP. c) Specific strength and specific modulus as a function of density for pristine and ITAP-40 yarns. Arrows point from pristine yarn to ITAP yarn results. d) Comparison of specific static torque generated in pristine yarn, τ(pristine), and in the ITAP-30 yarn, τ(ITAP), as a result of applying a tensile stress. The error bars are for one standard derivation, based on 5 or 7 measurements.

(1.27 g cm^{-3}) provided the highest strength (2.0 GPa), modulus (170 GPa), specific strength (1.6 N tex^{-1}), and specific modulus (137 N tex^{-1}) for the ITAP-40 yarns. However, the lowest-density precursor yarn (0.49 g cm^{-3}) underwent the highest increase in strength (2.58-fold) and modulus (12.0-fold) and in specific strength (1.4-fold) and specific modulus (6.4-fold). Density increase was observed for the pristine yarns having densities of 0.49, 0.82, and 1.08 g cm^{-3} after ITAP-40 (Figure 2b,c). Since their density is already ≈80% the maximum theoretical yarn density (Supporting Information), the highest-density yarns showed a very small density change after ITAP-40. Increasing the gauge length used above from 6 to 25.4 mm resulted in an almost identical mechanical strength (Figure S13, Supporting Information).

What is the origin of this increase in mechanical properties as a result of the ITAP? Long-term, high-temperature annealing can remove impurities and heal defects on CNTs,[30,31] thus improving their mechanical properties.[32] However, application of ITAP-30 at ≈2000 °C for 10 s significantly improved the strengths and moduli of MWNT yarns (Figure S4, Supporting Information), but did not much improve their graphitization (Figure S8, Supporting Information), indicating that the mechanical property enhancements can be mainly attributed to enhanced inter-nanotube connections rather than nanotube graphitization. In addition to improving the strength and modulus by increasing yarn density, the ITAP increased specific strength and specific modulus compared to the pristine yarns having the same density (Figure 2b,c). Based on the following experiment and simulation results, we attribute these increases in specific strength and specific modulus to inter-nanotube cross-links.

The torque needed to prevent untwist is near zero for the ITAP-40 yarn (Figure 2d), since the torque generated by yarn untwist is balanced by the ITAP-generated inter-nanotube connections. This explains the stability of ITAP yarns with respect to untwist and snarling. When tensile stress is applied to the ITAP yarns, this force balance is eliminated, so an external torque must be applied to prevent yarn untwist. Figure 2d shows the static torque needed to counter yarn untwist as a function of applied tensile stress for the pristine yarn and the ITAP-30 yarn (Supporting Information), both of which had 33 μm diameter and 36° bias angle. For the lowest applied tensile stress (13 MPa), the torque needed to prevent untwist was ≈10 times lower for the ITAP yarn than for the pristine twisted yarn. Although increasing the tensile stress led to the torque increase for both yarns, the torque for the ITAP yarn was still only ≈50% of that for the pristine yarn.

When the applied tensile stress is torsionally unconstrained, pristine yarns untwists many more turns than ITAP yarns. For example, a 2-gram freely rotating load caused considerable untwist to a 20-μm diameter pristine twisted yarn but negligible untwist for the corresponding ITAP-30 yarn (Movie S1, Supporting Information). Increasing the load to 5 grams caused both of the yarns to untwist, but the pristine yarn untwisted seven times the turns the ITAP-30 yarn did. After removing the load, the ITAP-30 yarn fully retwisted back while the pristine yarn only retwisted 16% of its untwist turns. These comparison results indicate that the ITAP-generated inter-nanotube connections provided a returning spring, which enabled the ITAP yarns a high reversibility of untwisting/twisting within a proper load range. This property is of great importance for solving the unwanted untwist problem for torsional actuators. Further increasing this load to 10 gram led to the fracture of the ITAP-30 yarn after untwisting about 12% of the inserted twist. In contrast, the pristine yarn stopped untwisting without yarn breakage after rotating 60% of the inserted twist. The SEM images in Figure S14 (Supporting Information) show that untwist-induced cracks were uniformly distributed along the axis of the pristine yarn (Figure S14a, Supporting Information) but occurred only in the vicinity of yarn rupture for the ITAP-30 yarn (Figure S14b, Supporting Information).

Additional support for the possibility of inter-nanotube cross-links is provided by the following observations that the ITAP yarns have long-term structural and mechanical stability in chlorosulfonic acid (**Figure 3**), whose strong protonation ability ordinarily debundles carbon single wall nanotubes and MWNTs and causes CNT structures to swell and then disintegrate.[33,34] Upon immersion in chlorosulfonic acid for 4–5 min, the pristine twisted yarn swelled, untwisted, and became disordered (Figure 3a,c,e), which led to a tenfold decrease in yarn strength and a 5.8-fold decrease in modulus (measured after removal of the acid, Figure 3f). In contrast, an ITAP-25 yarn remained aligned and densely packed, did not swell, and retained 82% of its modulus and 90% of its strength after immersion in chlorosulfonic acid for 4–5 min (Figure 3a,b,d,f). These results suggest that ITAP-induced cross-linking prohibited the chlorosulfonic acid from substantially penetrating and expanding the ITAP yarns.

The ITAP yarns also showed increased resistance to oxidation in the air compared to pristine yarns. Annealing in air at 500 °C for 10 min decreased the strength of a pristine yarn by about 38%. In contrast, the corresponding ITAP-40 yarn survived in this oxidation process without undergoing a significant decrease in strength (Figure S15, Supporting Information). This increase in oxidative stability is apparently not due to a density increase during the ITAP since the pristine yarn and the ITAP-40 yarn had similar densities (1.25 g cm^{-3}).

Unless a torsional return spring is provided, previously described single-ply, twist-spun or coiled CNT yarns cannot be used as a reversible torsional artificial muscle.[1–3] The solution used was to two-end torsionally tether the yarn and to actuate only half of its length so that the nonactuated length functioned as a torsional return spring.[1] However, the disadvantage of this approach is that it decreases the yarn length that contributes to actuation, and thereby makes the resulting torsional motors unnecessarily long. Instead of using single-ply coiled yarn, Peng and co-workers utilized a helical thread prepared by coiling multiplied straight CNT yarns, which were relatively stable and showed reversible actuation of rotating a lightweight rotor attached at the thread end when driven by solvent infiltration.[3] While solid guests in previously described hybrid muscles could act as internal torsional return springs to enable reversible actuation, this restricts the type of yarn guest that can be used, thereby eliminating the possibility of using fully actuated, nontethered, single-ply yarns as intelligent actuating sensors that can open and close valves in response to vapors, liquids, and liquid-delivered biological materials. For these reasons, previously described tensile muscles for controlling valves

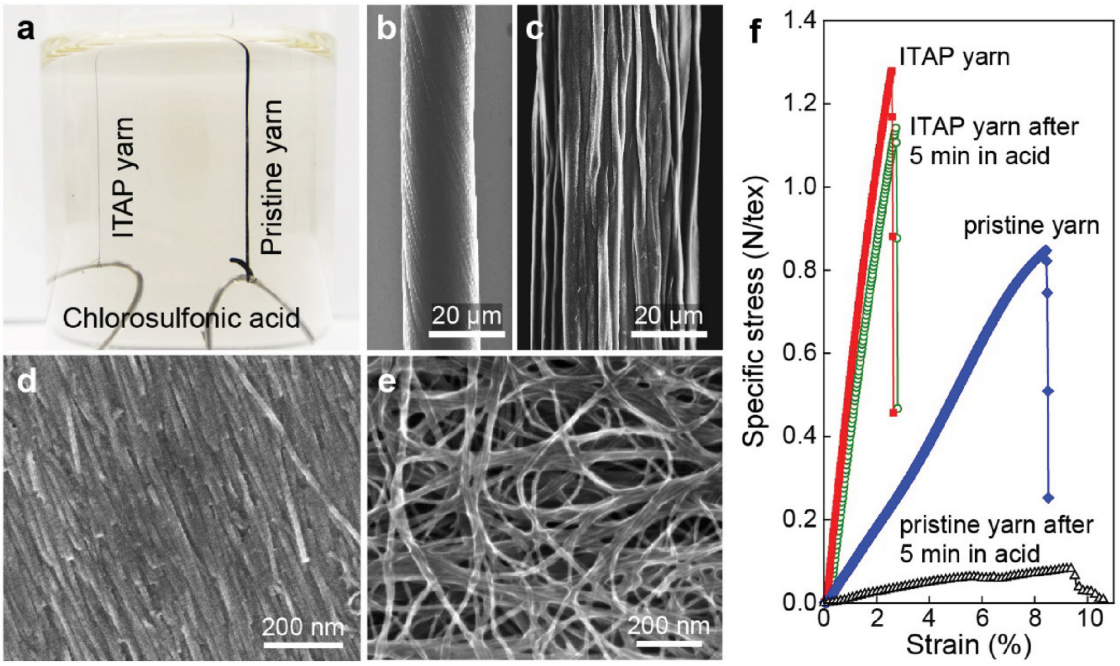

Figure 3. a) Photograph of pristine twisted yarn and thereby derived ITAP-30 yarn after 5 min immersion in chlorosulphonic acid and b,c) low-resolution and d,e) high-resolution SEM images of b,d) chlorosulfonic acid-treated ITAP-30 twisted yarn and c,e) pristine twisted yarns after 4 min immersion in this acid and subsequent drying. f) Comparison of strength–strain curves for the pristine and ITAP-25 yarns before and after immersion in chlorosulfonic acid for 5 min and subsequent removal of this chlorosulfonic acid from the yarns. This removal of the acid was accomplished by sequential washing of the fiber in ice water and ethanol, and then evaporation of the ethanol in air at 100 °C.

in response to a liquid composition or harvesting electrical energy by using liquid waste streams having different compositions were two-end tethered to prevent torsional rotation.[12]

We show here that fast, reversible torsional and tensile actuation of guest-free ITAP yarns can be simultaneously realized in response to the absorption and desorption of organic vapors, such as acetone and ethanol (Supporting Information). No external torsional tethering or external return spring was needed, since ITAP-produced inter-nanotube connections acted as internal springs. The actuator simply comprises a one-end-supported, coiled, single-ply ITAP yarn muscle that has attached on its opposite end a heavy rotor (**Figure 4**a). Vapor absorption induced yarn volume expansion and caused the coiled ITAP yarn to untwist and contract in length, while vapor desorption made the yarn retwist and increase in length due to the internal spring. In contrast, pristine coiled yarns irreversibly untwisted when in the same configuration (Movie S2, Supporting Information).

When exposed to acetone vapor, a 24-mm-long, 100-μm-thick coiled ITAP yarn reversibly rotated a 6100 times heavier rotor by 630° (corresponding to a rotation of 26° per millimeter of muscle length). The maximum rotational speed of the rotor was 44 rpm, and the muscle lifted a weight corresponding to a 2.9 MPa load by about 0.7% of the yarn length (Figure S16, Supporting Information). The torsional angle oscillations in Figure 4a were due to the cyclic interconversion of the kinetic energy of the rotating rotor to the strain energy of rotor rotation as the rotors kinetic energy was progressively damped. These oscillations in torsional actuation were eliminated by operating the muscle at near torsional resonance by using a vapor on/off cycle frequency of 0.18 Hz (Movie S3, Supporting Information). Such resonant operation increased torsional actuator stroke and maximum rotor speed by factors of 2.6 and 3.5, respectively (to 52° mm^{-1} and 160 rpm, respectively). It also caused a phase shift of about 1/4 period between the curves for the time dependence of torsional and tensile strokes (Figure 4b), which provided near coincidence of the peaks in rotor speed and tensile stroke.

Reflecting the mechanical robustness of the coiled ITAP yarn to irreversible yarn untwist, reversible torsional and tensile actuation was obtained even when high-weight torsional rotors were deployed. While increasing yarn stress from 2.9 to 13.5 MPa (corresponding to 28 396 times the muscle weight) by increasing rotor weight did not dramatically change torsional actuation stroke (Figure 4c), the corresponding increase of moment of inertia for the rotor (from 8.0×10^{-9} to 4.8×10^{-7} kg m^2) decreased maximum rotation speed from 155 to 51 rpm (Figure 4d). Analysis of the results in Figure 4c provides the stress dependency for actuation as shown in Figure 4d, where the specific torque generated by actuation was derived from rotor moment of inertia and rotor acceleration during vapor-powered forward actuation.[1] Independent of the stress applied by the rotor, the maximum speed obtained during yarn twist and untwist were nearly identical. Even though the achieved torsional speeds are smaller than that for previously reported CNT yarn actuators,[1–3] the obtained maximum torque (4.12 N m per kilogram of the yarn mass) of the ITAP yarn was several times the torque of electrochemically and absorption driven CNT muscles,[1,3,35] 50 times the torque generated by the moisture-driven graphene-yarn torsional actuator,[36] and comparable to the static torque of the

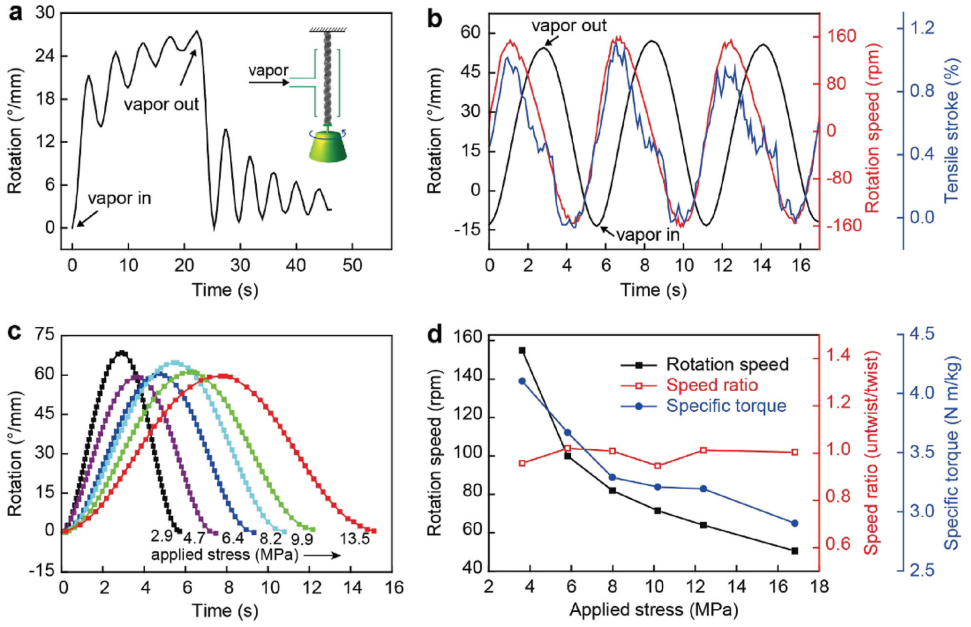

Figure 4. a) Weight rotation in degrees (normalized to yarn length) versus time for a one-end-tethered, coiled ITAP yarn (inset, with 24 mm length and 100 μm yarn diameter) when driven by acetone vapor absorption/desorption. The weight provides a 2.9 MPa stress on the yarn. b) Weight rotation (black), rotation speed (red) and tensile actuation (blue) versus time for the ITAP yarn when excited by a vapor on/off cycle frequency of 0.18 Hz. c) Resonant torsional rotation stroke versus time when different weight rotors were deployed, which provided the indicated stresses. d) Maximum rotation speed, the ratio of maximum untwisting and twisting speed, and specific torque versus weight-induced tensile stress extracted from the data in panel (c) for the coiled ITAP yarn.

electrothermally driven wax-filled CNT muscles.[2] Moreover, such ITAP yarns showed highly reversible torsional actuation (Figure S17, Supporting Information).

Previous experimental and simulation results have demonstrated that nanocarbons such as CNTs, amorphous carbon, and graphene can undergo covalent bond reconfiguration at high temperatures.[37–40] These covalent structure changes, such as inter-nanotube covalent bonding, nanotube coalescence, and formation of graphitic nanoribbons, can be facilitated by the presence of amorphous carbon and defects in the carbon sidewalls.[41,42] Since even a very low concentration of cross-links between nanotubes could profoundly influence properties and the yarn structure is very complex, direct experimental observation of inter-nanotube covalent bonding was not presently possible (Figure S11, Supporting Information). Hence, we conducted molecular dynamics simulations using the large-scale atomic/molecular massively parallel simulator (LAMMPS) code to gain insight into the nature of cross-links possibly formed during the ITAP (Supporting Information).[43] The investigated model structure consisted of 5-nm-long, 8.8-nm-thick DWNTs having chiral indices of (65, 65) and (60, 60) for the outer shells and inner shells, respectively (Figure S18a, Supporting Information). Random vacancy defects generated by removing 5% of the atoms at the outermost nanotube shells were introduced to approach the real case for our relatively defective MWNT yarns and facilitate fast reaction kinetics. By applying periodical boundary conditions, these DWNTs were hexagonally packed at van der Waals separations during the initial 300 K phase of the calculations.

When treated in a vacuum at 2500 K for about 50 ps followed by gradual cooling to 300 K, these DWNTs were covalently bonded through interstitial carbon atoms (Figure S18b, Supporting Information). Hybridization types of sp, sp^2, and sp^3 were observed for these interstitial atoms and the types of connection bonds include sp^2–sp, sp^2–sp^2, and sp^2–sp^3, which is consistent with the literature results.[44] The details of the bonding structures were shown in Figure S18b in the Supporting Information. Since amorphous carbon and defects on CNTs can have similar bond structures, it is difficult to spectroscopically identify cross-links. However, it is noteworthy that the Raman spectra of the ITAP-30 yarn annealed for 2 h showed a much lower G/D intensity ratio than the yarn annealed for the same time, but without applying a load.

We have shown that the fast, commercially applicable ITAP provides remarkable improvements in the properties of twist-spun and coiled CNT yarns. These improvements include major increases in yarn strength and modulus, increases in oxidative stability, and stability to an acid that powerfully protonates yarns and makes them unusable, and the setting of inserted twist for various applications. Since twist retention during nanotube yarn weaving is extremely important, especially for the warp yarns that are highly strained during weaving, this twist setting can be important for the commercial production of nanotube textiles for energy storage, harvesting and conversion, sensing, and actuation. This twist retention enables the first single-ply, guest-free, CNT yarns that can serve as reversible tensile and torsional muscles without the need for external return springs that degrade performance metrics.

Experimental Section

Incandescent Tension Annealing Process: The ITAP was conducted at 5.5×10^{-6} bar within a vertically placed cylindrical tube. An approximately

20-cm-long twist-spun MWNT yarn was wrapped around two 500 μm diameter molybdenum electrodes and an electrical current was applied through these electrodes to heat the yarn (or an assembly of parallel yarns) to ≈2000 °C. Before incandescently heating the yarns, a small current was applied to remove the oxygen absorbed on the MWNTs. For precursor yarns having a diameter smaller than 20 μm, precise measurement of the electrothermally achieved temperature was difficult. To accomplish this, we measured temperature spectroscopically based on black body radiation and used measurements of resistance as a function of temperature to calibrate the spectroscopically determined temperature. We applied tensile stress by hanging various size weights on the MWNT yarns through the bottom molybdenum hook electrode during high-temperature annealing. The maximum applied stress was about 40% of the fracture strength of the twisted pristine MWNT yarns. Application of higher stresses led to yarn rupture, likely because the strength of the pristine yarn at high temperatures was below its room-temperature strength. For the coiled yarns used for actuators, the stress applied during ITAP was sufficient to avoid yarn from snarling. Reported stresses are normalized with respect to the unstrained diameter of the twist-inserted, noncoiled yarn. Unless otherwise mentioned, the twisted and the coiled MWNT yarns were annealed for 2 min at ≈2000 °C. After the current interruption at the end of annealing, the yarns rapidly cooled to room temperature in vacuum.

Supporting Information

Supporting Information is available from the Wiley Online Library or from the author.

Acknowledgements

This work was supported by the Air Force Office of Scientific Research grants FA9550-12-1-0035, FA9550-12-1-0211, and FA2386-13-1-4119; Robert A. Welch Foundation grant AT-0029; National Science Foundation grant CMMI1335204; Office of Naval Research MURI grant NOOD14-11-1-0691; and the Army grant W91CBR-13-C-0037. The authors thank X. M. Tao and T. G. Xu for useful comments and W. W. Jiang for assistance in generating the CNT models.
Note: The presentation of the author name M. Jung de Andrade was corrected in the affiliations on August 11, 2016, after initial publication online.

Received: February 1, 2016
Revised: April 20, 2016
Published online: May 17, 2016

[1] J. Foroughi, G. M. Spinks, G. G. Wallace, J. Oh, M. E. Kozlov, S. L. Fang, T. Mirfakhrai, J. D. W. Madden, M. K. Shin, S. J. Kim, R. H. Baughman, *Science* **2011**, *334*, 494.
[2] M. D. Lima, N. Li, M. Jung de Andrade, S. Fang, J. Oh, G. M. Spinks, M. E. Kozlov, C. S. Haines, D. Suh, J. Foroughi, S. J. Kim, Y. Chen, T. Ware, M. K. Shin, L. D. Machado, A. F. Fonseca, J. D. Madden, W. E. Voit, D. S. Galvao, R. H. Baughman, *Science* **2012**, *338*,928.
[3] P. Chen, Y. Xu, S. He, X. Sun, S. Pan, J. Deng, D. Chen, H. Peng, *Nat. Nanotechnol.* **2015**, *10*, 1077.
[4] X. Chen, L. Qiu, J. Ren, G. Guan, H. Lin, Z. Zhang, P. Chen, Y. Wang, H. Peng, *Adv. Mater.* **2013**, *25*, 6436.
[5] W. Weng, Q. Sun, Y. Zhang, H. Lin, J. Ren, X. Lu, M. Wang, H. Peng, *Nano Lett.* **2014**, *14*, 3432.
[6] M. D. Lima, S. Fang, X. Lepro, C. Lewis, R. Ovalle-Robles, J. Carretero-Gonzalez, E. Castillo-Martinez, M. E. Kozlov, J. Oh, N. Rawat, C. S. Haines, M. H. Haque, V. Aare, S. Stoughton, A. A. Zakhidov, R. H. Baughman, *Science* **2011**, *331*, 51.
[7] W. Lu, M. Zu, J. H. Byun, B. S. Kim, T. W. Chou, *Adv. Mater.* **2012**, *24*, 1805.
[8] K. Liu, Y. Sun, X. Lin, R. Zhou, J. Wang, S. Fan, K. Jiang, *ACS Nano* **2010**, *4*, 5827.
[9] M. Zhang, K. R. Atkinson, R. H. Baughman, *Science* **2004**, *306*, 1358.
[10] Y. Shang, X. He, Y. Li, L. Zhang, Z. Li, C. Ji, E. Shi, P. Li, K. Zhu, Q. Peng, C. Wang, X. Zhang, R. Wang, J. Wei, K. Wang, H. Zhu, D. Wu, A. Cao, *Adv. Mater.* **2012**, *24*, 2896.
[11] Y. Li, Y. Shang, X. He, Q. Peng, S. Du, E. Shi, S. Wu, Z. Li, P. Li, A. Cao, *ACS Nano* **2013**, *7*, 8128.
[12] M. D. Lima, M. W. Hussain, G. M. Spinks, S. Naficy, D. Hagenasr, J. S. Bykova, D. Tolly, R. H. Baughman, *Small* **2015**, *11*, 3113.
[13] B. Vigolo, A. Penicaud, C. Coulon, C. Sauder, R. Pailler, C. Journet, P. Bernier, P. Poulin, *Science* **2000**, *290*, 1331.
[14] L. M. Ericson, H. Fan, H. Peng, V. A. Davis, W. Zhou, J. Sulpizio, Y. Wang, R. Booker, J. Vavro, C. Guthy, A. N. Parra-Vasquez, M. J. Kim, S. Ramesh, R. K. Saini, C. Kittrell, G. Lavin, H. Schmidt, W. W. Adams, W. E. Billups, M. Pasquali, W. F. Hwang, R. H. Hauge, J. E. Fischer, R. E. Smalley, *Science* **2004**, *305*, 1447.
[15] N. Behabtu, C. C. Young, D. E. Tsentalovich, O. Kleinerman, X. Wang, A. W. Ma, E. A. Bengio, R. F. ter Waarbeek, J. J. de Jong, R. E. Hoogerwerf, *Science* **2013**, *339*, 182.
[16] K. L. Jiang, Q. Q. Li, S. S. Fan, *Nature* **2002**, *419*, 801.
[17] Y. L. Li, I. A. Kinloch, A. H. Windle, *Science* **2004**, *304*, 276.
[18] X. F. Zhang, Q. W. Li, T. G. Holesinger, P. N. Arendt, J. Y. Huang, P. D. Kirven, T. G. Clapp, R. F. DePaula, X. Z. Liao, Y. H. Zhao, L. X. Zheng, D. E. Peterson, Y. T. Zhu, *Adv. Mater.* **2007**, *19*, 4198.
[19] X. B. Zhang, K. L. Jiang, C. Teng, P. Liu, L. Zhang, J. Kong, T. H. Zhang, Q. Q. Li, S. S. Fan, *Adv. Mater.* **2006**, *18*, 1505.
[20] C. Jayasinghe, S. Chakrabarti, M. J. Schulz, V. Shanov, *J. Mater. Res.* **2011**, *26*, 645.
[21] N. Behabtu, M. J. Green, M. Pasquali, *Nano Today* **2008**, *3*, 24.
[22] Y. Shang, C. Hua, W. Xu, X. Hu, Y. Wang, Y. Zhou, Y. Zhang, X. Li, A. Cao, *Nano Lett.* **2016**, *16*, 1768.
[23] T. Filleter, H. D. Espinosa, *Carbon* **2013**, *56*, 1.
[24] C. Fang, J. Zhao, J. Jia, Z. Zhang, X. Zhang, Q. Li, *Appl. Phys. Lett.* **2010**, *97*, 181906.
[25] S. Ryu, Y. Lee, J.-W. Hwang, S. Hong, C. Kim, T. G. Park, H. Lee, S. H. Hong, *Adv. Mater.* **2011**, *23*, 1971.
[26] A. Kis, G. Csanyi, J. P. Salvetat, T.-N. Lee, E. Couteau, A. J. Kulik, W. Benoit, J. Brugger, L. Forro, *Nat. Mater.* **2004**, *3*, 153.
[27] A. V. Krasheninnikov, F. Banhart, *Nat. Mater.* **2007**, *6*, 723.
[28] T. Filleter, R. Bernal, S. Li, H. D. Espinosa, *Adv. Mater.* **2011**, *23*, 2855.
[29] M. Miao, S. C. Hawkins, J. Y. Cai, T. R. Gengenbach, R. Knott, C. P. Huynh, *Carbon* **2011**, *49*, 4940.
[30] W. Huang, Y. Wang, G. Luo, F. Wei, *Carbon* **2003**, *41*, 2585.
[31] K. Behler, S. Osswald, H. Ye, S. Dimovski, Y. Gogotsi, *J. Nanopart. Res.* **2006**, *8*, 615.
[32] G. Yamamoto, K. Shirasu, Y. Nozaka, Y. Sato, T. Takagi, T. Hashida, *Carbon* **2014**, *66*, 219.
[33] V. A. Davis, A. N. Parra-Vasquez, M. J. Green, P. K. Rai, N. Behabtu, V. Prieto, R. D. Booker, J. Schmidt, E. Kesselman, W. Zhou, H. Fan, W. W. Adams, R. H. Hauge, J. E. Fischer, Y. Cohen, Y. Talmon, R. E. Smalley, M. Pasquali, *Nat. Nanotechnol.* **2009**, *4*, 830.
[34] A. N. Parra-Vasquez, N. Behabtu, M. J. Green, C. L. Pint, C. C. Young, J. Schmidt, E. Kesselman, A. Goyal, P. M. Ajayan, Y. Cohen, Y. Talmon, R. H. Hauge, M. Pasquali, *ACS Nano* **2010**, *4*, 3969.
[35] S. He, P. Chen, L. Qiu, B. Wang, X. Sun, Y. Xu, H. Peng, *Angew. Chem. Int. Ed.* **2015**, *127*, 15093.
[36] H. H. Cheng, Y. Hu, F. Zhao, Z. L. Dong, Y. H. Wang, N. Chen, Z. P. Zhang, L. T. Qu, *Adv. Mater.* **2014**, *26*, 2909.

[37] M. Terrones, H. Terrones, F. Banhart, J. Charlier, P. M. Ajayan, *Science* **2000**, *288*, 1226.
[38] K. Asaka, M. Karita, Y. Saito, *Appl. Phys. Lett.* **2011**, *99*, 091907.
[39] F. Colonna, A. Fasolino, E. J. Meijer, *Phys. Rev. B* **2013**, *88*, 165416.
[40] J. Y. Huang, S. Chen, Z. F. Ren, G. Chen, M. S. Dresselhaus, *Nano Lett.* **2006**, *6*, 1699.
[41] H. R. Gutierrez, U. J. Kim, J. P. Kim, P. C. Eklund, *Nano Lett.* **2005**, *5*, 2195.
[42] E. Salonen, A. Krasheninnikov, K. Nordlund, *Nucl. Instrum. Methods Phys. Res., Sect. B* **2002**, *193*, 603.
[43] S. Plimpton, *J. Comput. Phys.* **1995**, *117*, 1.
[44] N. P. O'Brien, M. A. McCarthy, W. A. Curtin, *Carbon* **2013**, *51*, 173.